AMERICAN SCIENTIFIC PUBLISHERS

Science of Advanced Materials
Vol. 9, pp. 1–10, 2017
www.aspbs.com/sam

ARTICLE

Osteogenic Comparison on Selective Laser Melting Printed and Sandblasting-Acid-Etching Ti Substrates for Customized Implant Applications

Mengke Wang[1,2,†], Tong Chen[1,2,†], Songhe Lu[1,2], Yijiao Zhao[2], Hu Chen[2], Yuwei Wu[1,2,*], and Zhihui Tang[1,2,*]

[1] *2nd Dental Center, School and Hospital of Stomatology, Peking University, Beijing, 100081, People's Republic of China*
[2] *National Engineering Laboratory for Digital and Material Technology of Stomatology, School and Hospital of Stomatology, Peking University, Beijing, 100081, People's Republic of China*

ABSTRACT

Implants treated by sandblasting acid etching (SLA) have been demonstrated to be capable of hastening the osseointegration process. However, they suffer from some shortcomings, which include contamination by the grit-blasting materials and residual acid solution, as well as limited satisfaction of certain requirements for oral use. As an alternative procedure that enables the fabrication of customized implants with complex geometries, the use of selective laser melting (SLM) to fabricate implants has recently drawn considerable attention. In the present work, SLM-printed substrates were compared with commercially available SLA-treated plates in terms of their surface characteristics and biological performance. The wettability and roughness of SLM-printed substrates were found to be significantly better. Moreover, *in vitro* evaluations revealed that the SLM surface facilitated the attachment and proliferation of human bone marrow mesenchymal stem cells (hBMSCs), and induced accelerated osteogenic progression, as indicated by the observed increased alkaline phosphatase (ALP) activity, elevated expression of osteo-related mRNA, and intense calcium deposition. Overall, the SLM-based substrates exhibited suitable cytocompatibility and osteophilic properties, which are expected to enhance *in vivo* bone-implant contact and osseointegration. A comprehensively optimized SLM-printed substrate mimics a more osteophilic environment and affords an alternative means of producing customized implants in oral implantology.

KEYWORDS: Titanium, Selective Laser Melting (SLM), Sandblasting and Acid Etching (SLA), Osteogenic Differentiation, Cytocompatibility.

1. INTRODUCTION

Titanium (Ti) is a well-established implant material in dentistry owing to its excellent mechanical properties, superior corrosion resistance, and favorable biocompatibility with bone.[1,2] However, the long-term stability of Ti implants significantly depends on early and effective osseointegration, which is in turn substantially determined by the surface properties of the implant material, including the topography, chemistry, and wettability.[3] Toward inducing early peri-implant bone formation, a series of surface treatments, such as grit-blasting, acid-etching, and anodization, have been used to optimize the physical and chemical properties of implant surfaces.[4]

Among these methods, sandblasting acid etching (SLA) treatment is a relatively simple and effective technique and has been successfully employed clinically for decades.[4] An SLA-treated surface with suitable roughness and micro/nano-textures, which guarantee a stable bone-implant interface, has been demonstrated to enhance *in vitro* cellular response and *in vivo* bone formation.[5] However, contamination by the grit-blasting material (e.g., Al_2O_3 particles) and residual acid solution on the implant surface may hamper the osseointegration process.[6] Moreover, commercially available standard SLA implants which are produced by traditional processing technologies such as casting and forging, only come with cylindrical or tapered geometries with limited lengths and diameters. They thus do not always satisfy individual oral conditions.[7]

Recently, selective laser melting (SLM), which is one of the emerging metal-based additive manufacturing (AM) techniques, has attracted considerable interest for use

*Authors to whom correspondence should be addressed.
Emails: yuweiwu@bjmu.edu.cn, zhihui_tang@126.com
†These two authors contributed equally to this work.
Received: xx Xxxx xxxx
Accepted: xx Xxxx xxxx

ARTICLE

in the one-step fabrication of near-net-shaped and customized implants based on virtual three-dimensional (3D) model data. Compared to traditional methods, SLM offers many advantages relevant to dental implants, including higher material utilization, minimal machining, shorter production time, and almost no geometric restriction, which enables the fabrication of implants with controlled complex geometry, almost without the need for post-processing.[8,9] In addition, due to its high precision and excellent performance, SLM promises to afford implants with comparable or even better mechanical behavior, including excellent fatigue properties, yield strength, ultimate tensile strengths, and hardness compared to those processed by traditional methods.[10–12] Although slightly inferior to that of their counterparts prepared by traditional methods,[13] the corrosion resistance of the SLM-based products, another critical property for their clinical application, could be enhanced via adjusting the scan strategies and build orientations in the process of SLM.[14] What's more, from a biomimetic viewpoint, SLM-based dental implants tailored to individual patients not only exhibit better preservation of hard and soft tissues but also reduce the rehabilitation time and satisfy the anatomical and functional requirements for dental implants.

Despite the above-mentioned advantages, there is still the need to ensure that the synthetical properties of SLM-fabricated components are of acceptable standards. Although there are many issues needing further investigation, the first requirement is to evaluate the *in vitro* biological performance of SLM-fabricated components before proceeding to animal studies and clinical tests. To the best of our knowledge, there has been no previous systematic experimental study that was dedicated to evaluating the differences between SLM-printed and wrought SLA-treated Ti substrates, especially with regard to their biological performance. In the present study, the surface characteristics, cytocompatibility and osteophilic property of SLM-based substrates were carefully assessed and compared with those of commercial SLA-treated implants with known osseointegration and clinical performance, as a critical step toward the application of SLM-based oral implants.

2. EXPERIMENTAL SECTION

2.1. Preparation of Titanium Samples

Commercially pure titanium disks (Grade 4, Leiden, Beijing, China) were polished on one side using a series of silicon carbide sandpapers (200, 400, 600, 800 and 2000 μm) and then further polished for 3 min using 6 and 1 μm diamond paste. The samples, which were polished to a mirror finish, were tagged cp-Ti and used as a negative control. Some of the cp-Ti samples were further sandblasted with 250–500 μm Al_2O_3 particles at 5 bar, and this was followed by etching for several minutes in a mixture of hydrochloric and sulfuric acids heated above 100 °C (proprietary process of Institut Straumann AG). This was done to produce "sandblasted-large-grit-acid-etched" discs, which were tagged SLA-Ti.

The employed 3D printing Ti samples, which were provided by Jing Sun Medical Technology Services LTD. (Shanghai, China), were manufactured in a selective laser melting machine (Mlab Cusing R, Concept Laser GmbH, Lichtenfels, Germany) under an argon atmosphere using optimized parameters. The parameters used were a laser power of 100 W, scanning speed of 900 mm/s, spot size of 50 μm, and layer thickness of 30 μm. After fabrication, the samples were annealed at 1000 °C (10 °C/min) for 1 h and slowly cooled to 70 °C inside the furnace under an argon shield to eliminate internal stress. These samples were tagged SLM-Ti.

Each of the above Ti sample types comprised disks of two sizes, namely, $15 \times 15 \times 1$ mm (particularly used for surface characterization, cell counting kit-8 (CCK-8), immunofluorescence, and alkaline phosphatase (ALP) assay), and $30 \times 30 \times 1$ mm (particularly used for real-time polymerase chain reaction (PCR) and Alizarin Red S staining assays). After the surface treatments, all the samples were ultrasonically cleaned sequentially in acetone, absolute alcohol and distilled water for 20 min each, and then sterilized in an autoclave at 120 °C for 30 min.

2.2. Surface Characterization

The cp-Ti, SLA-Ti, and SLM-Ti samples were examined after sterilization by using a variety of surface-sensitive techniques as described below. The surface morphology was examined using a field emission scanning electron microscope (FE-SEM, JSM-6500 F, JEOL, Tokyo, Japan) under an acceleration voltage of 20 kV. The surface roughness was determined by separately examining 10 different areas on each sample under a laser scanning confocal microscope (LSCM, VK-X100K, KEYENCE, Osaka, Japan). Each sample was scanned to obtain the 3D surface profile. The obtained images were analyzed using the VK-H1XP software to determine the average roughness (Ra). In addition, the surface chemical composition of each sample was analyzed by X-ray photoelectron spectroscopy (XPS, Kratos Analytical Ltd., UK). Both the survey and high-resolution spectra were obtained. The obtained spectra were curve-fitted using a computer-assisted Lorentzian–Gaussian peak model. The binding energies were calibrated by the C 1*s* hydrocarbon peak at about 285 eV. A quantitative analysis and curve fitting were also performed using the CasaXPS software package. The crystalline structures were examined and compared by an X-ray diffractometer (XRD-6100, SHIMADZU Corp., Kyoto, Japan) using a Cu target as the radiation source at 40 kV and 100 mA. Diffraction angle (2θ) values of 20–60° in steps of 0.02° and a scan speed of 4° 2θ/min were employed. The surface hydrophilicity was evaluated

by measuring the water contact angle at ambient temperature using a contact angle goniometer (OCA20, DATAPHYSICS, Filderstadt, Germany) based on the sessile drop method. Six distinct spots on three parallel specimens were used to provide an average and standard deviation for each sample type.

2.3. Cell Culture and Osteogenic Differentiation

Human bone marrow mesenchymal stem cells (hBMSCs) purchased from ScienCell (California, America) were cultured in standard tissue culture dishes using a proliferation medium (PM) consisting of 90% α-minimal essential medium (α-MEM, Gibco, USA), 10% fetal bovine serum (FBS, Gibco), and 1% penicillin-streptomycin (Invitrogen, Carlsbad, CA). The cultures were maintained at 37 °C in a humidified 5% CO_2 incubator (MCO-18AIC, Japan). The cells were fed every 2 days and passaged at a split ratio of 1:3 upon 90% confluency by exposure to 0.25% trypsin-EDTA solution (Gibco) for 30 s.

All the Ti discs were then autoclaved, rinsed with sterile phosphate-buffered saline (PBS), and transferred into new tissue culture plates. Prior to cell seeding, the specimens were equilibrated in PM for 10 min. The hBMSCs were subsequently drop-seeded on the substrates with a density of 5×10^4 cells/mL and incubated statically for at least 1 h to allow cell attachment. After 1 day, the medium was replaced with an osteogenic-inducing medium (OM), which was prepared by adding 10^{-8} M dexamethasone (DEX, Sigma-Aldrich), 5 μg/mL ascorbic acid (AA, Sigma-Aldrich), and 10 mM β-glycerophosphate (β-GP, Sigma-Aldrich) to the PM. The culture medium was changed every 2 days, with the entire process lasting 21 days. Day 1 was set as the day on which the osteogenic induction commenced. To compare the osteogenic outcome, hBMSCs seeded on tissue culture plastic (TCP) and smooth titanium substrate (cp-Ti) served as the positive and negative controls, respectively. hBMSCs cultured with PM was also used as control.

2.4. Immunofluorescence

hBMSCs cultured in PM for 6 and 24 h were separately fixed with 4 v/v% paraformaldehyde for 15 min and permeabilized with 0.1 v/v% Triton X-100 (Solarbio, Beijing, China) for 5 min at room temperature. Subsequently, fluorescein isothiocyanate (FITC)-labeled phalloidin (5 μg/mL) and 6-diamidino-2-phenylindole (DAPI, 10 μg/mL) were used to counterstain the F-actin and cell nuclei, respectively. Each staining step was followed by three washes in PBS. The stained signals in the cells were immediately visualized by a laser confocal microscope (LSM5, Carl Zeiss, Germany).

2.5. Cell Proliferation Assay

After 1, 4, and 7 days of incubation, the disks were transferred into new 12-well plates to evaluate the cell proliferation by a cell counting kit-8 assay (CCK-8, Dojindo, Japan). Briefly, at desired time intervals, CCK-8 solution was added in each well at a proportion of 1:10 (v/v), followed by 2 h incubation in darkness. Thereafter, 100 μL of supernatant from each well was transferred into new 96-well cell culture plates. The optical densities (ODs) of the supernatants were measured using a microplate reader (Model 680, Bio-Rad, Canada) at 450 nm. The average and standard deviation were determined for six parallel specimens from each supernatant group.

2.6. Alkaline Phosphate (ALP) Assay

The alkaline phosphatase (ALP) activity of hBMSCs, an early indicator of osteogenesis, was quantified by an assay reagent kit (NJJC-BIO, Nanjing, China). Briefly, after 7 and 14 days of cultivation the cell layers were washed with frozen PBS and scraped off from the surfaces using 200 μL 1% Triton X-100 (lysis solution) per well. After sonication and centrifugation at 12000 rcf for 30 min, 30 μL of cell lysates was transferred from the wells to new 96-well plates, and cultivated with a carbonated buffer solution (50 μL, pH = 10) and substrate solution (4-aminoantipyrine, 50 μL) at 37 °C for 15 min. Thereafter, 150 μL of potassium ferricyanide was added to each well, and the production of *p*-nitrophenol was checked by measuring the absorbance at 405 nm. For normalization, the total protein concentration was determined by means of Pierce BCA protein assay kits (Thermo, USA) using bovine serum albumin (BSA) as the standard. The ALP activity was normalized and expressed in terms of the total protein content (U/gprot). ALP staining was done at desired time intervals using an ALP detection kit (CW-BIO, Beijing, China). Before the staining, the hBMSCs were fixed for 30 min using 95% cold ethanol, and this was followed by three washes in PBS. The staining was done over 15 min in accordance with the instructions of the kit manufacturers. Then cell attachment was visually scored by a scanner (ScanMaker i800, MICROTEK, Shanghai, China).

2.7. Quantitative Real-Time Polymerase Chain Reaction (qPCR)

To establish the difference between SLM-Ti and SLA-Ti at the molecular level, the respective variations of their specific gene expressions during osteogenesis were examined by quantitative real-time polymerase chain reaction (qPCR) after 7 and 14 days. After 7, and 14 days of cultivation, the entire mRNA in the cells on the tested substrates was extracted by TRIzol reagent (Invitrogen) and converted into cDNA using Revert Aid First Strand cDNA Synthesis Kit (Thermo). qPCR analysis was carried out with SYBR Green (Roche, USA) on an ABI 7500 RT-PCR machine (Applied Biosystems, USA). All the processes were implemented in triplicates, and glyceraldehyde 3-phosphate dehydrogenase (GAPDH) was used

Table I. Primer sequence (5′-3′) for the quantitative real-time PCR.

Name	Forward primer	Reverse primer
GAPDH	CGACAGTCAGCCGCATCTT	CCAATACGACCAAATCCGTTG
Run × 2	AGGAATGCGCCCTAAATCACT	ACCCAGAAGGCACAGACAGAAG
OCN	CTGGTCCCTCAGTCTCATTCC	GTCTCTTCACTACCTCGCTGC
Col1a1	AGACACTGGTGCTAAGGGAGAG	GACCAGCAACACCATCTGCG

as an internal control for PCR amplification. The specific primer sequences (5′-3′) used in this study are outlined in Table I. Primer sets (10 μM final concentration for each primer) were used in a volume of 20 μL per tube. The thermal profile of the PCR comprised of the following steps: 50 °C for 2 min, 95 °C for 10 min, followed by 40 cycles at 95 °C for 15 s and 60 °C for 1 min. The comparative CT (2^{-CT}) method was used to evaluate the differences among the fold gene expressions of the groups.

2.8. Alizarin Red S Staining and Mineralization Assays

Staining with Alizarin Red S (ARS) solution (Sigma-Aldrich) was used to determine the formation of mineralized nodule after 21 days of osteoinductive differentiation. ARS was dissolved in D.I. water at a concentration of 2 w/v%, and the pH was adjusted to 4.2. The cells on the substrates were washed with frozen PBS and fixed in 4% formalin for 10 min. The fixed cells were further washed with D.I. water to remove any salt residues, and ARS solution was then added to cover the entire surface of the wells containing the cells. After 20 min incubation at room temperature, the excess ARS was fully washed off with D.I. water. The calcium deposited on the substrates of each group was visually scored by a scanner (ScanMaker i800, MICROTEK, Shanghai, China). To quantify the matrix mineralization, the ARS-stained samples were immersed in cetylpyridinium chloride (1 w/v%, Sigma-Aldrich) overnight with shaking to dissolve the calcium mineral deposited by the cells. 100 μL of the supernatants were collected and placed in new 96-well cell culture plates and the OD_{562} was read by a microplate reader (Model 680, Bio-Rad).

2.9. Statistical Analysis

All the data are expressed as mean ± standard deviation. A one-way analysis of variance (ANOVA) Tukey post-hoc test was used to determine the significant differences among the groups, and p-values less than 0.05 were considered statistically significant.

3. RESULTS AND DISCUSSION

3.1. Surface Characterization of the Tested Ti Substrates

As shown in the scanning electron microscopy (SEM) micrographs (Fig. 1), the surface of the cp-Ti samples was relatively smooth on a microscopic scale, although some parallel scratches, presumably originating from the mechanical polishing process, were detected (Figs. 1(a–c)). After sandblasting and acid-etching, a large amount of micropits and microcavities with sharp edges were formed on the surfaces (Figs. 1(d–f)), resulting in a rougher honey-comb structure. In the case of the SLM-Ti printed by Ti powder, the SEM images (Figs. 1(g–i)) showed aggregates of global protuberances produced by the partial sintering of Ti particles on a microscopic scale closely bonded to the surface, resulting in a rougher, granulated surface pattern.

To further validate the SEM results, the average roughness (Ra) measured by laser scanning confocal microscopy (LSCM) (Fig. 2), was used to quantify the topography differences (Fig. 2(d)). In agreement with the SEM results, the cp-Ti samples were found to have a comparatively smooth texture with low Ra value (0.27 ± 0.03 μm). After SLA treatment, randomly distributed irregular wavy peaks (orange-red) and valleys (blue) were produced, resulting in an increased Ra value (2.92 ± 0.04 μm). 3D reconstructions of the SLM-Ti samples revealed the formation of a closely spaced and irregular lattice layer, which resulted in

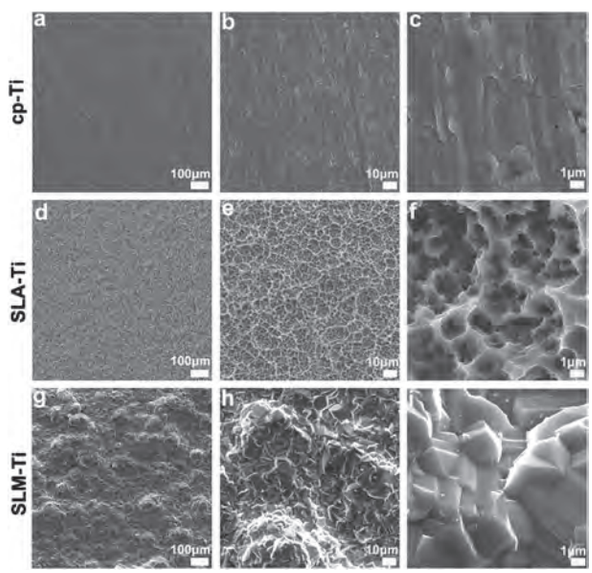

Fig. 1. SEM micrographs showing the surface morphology of the tested titanium discs (cp-Ti, SLA-Ti, and SLM-Ti) under different magnifications. (a, d, g) 100×; (b, e, h) 500×; (c, f, i) 5,000×.

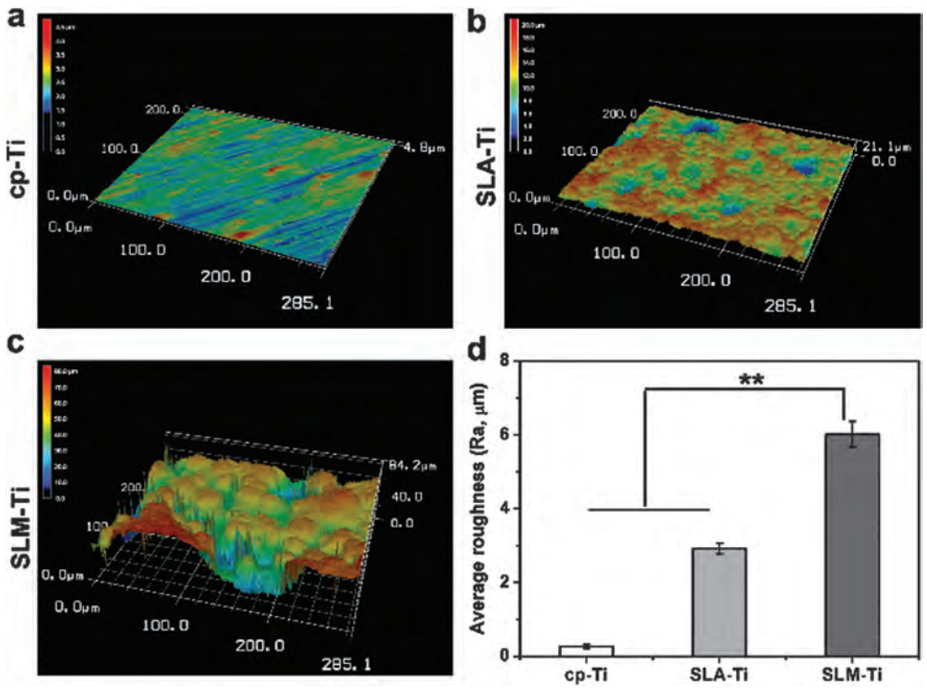

Fig. 2. 3D topographical reconstructions of cp-Ti (a), SLA-Ti (b), and SLM-Ti (c) substrates are presented using the laser scanning confocal microscope (LSCM). These images were analyzed with the VK-H1XP software to obtain the values of (d) average roughness (*Ra*). Data are displayed as means ± standard deviations ($n = 10$, $^{**}p < 0.01$).

a significantly rougher surface (6.02 ± 0.35 μm) compared to the cp-Ti and SLA-Ti samples ($p < 0.01$). As confirmed by the SEM and LSCM results, the SLM-printed surface was rougher and had an undulating texture. This is expected to enhance bone-implant contact and *in vitro* cell behavior.[15]

The implant chemical composition is also an important factor of cell-implant interaction.[16] The results of the semi-quantitative X-ray photoelectron spectroscopy (XPS) analyses (Figs. 3(a–b)) showed that all the disks exhibited major peaks at Ti 2*p*, O 1*s*, and C 1*s*, and also contained traces of *N*. The predominant elements, Ti and O, probably originated from the superficial native TiO_2 layer, while the C signals may be attributed to unavoidable exposure to the ambient environment.[17] Successful SLA was indicated by an increase in the O 1*s* content, and corresponding decrease in the C 1*s* content from 45.66% to 40.03%, as shown in Figure 3(b). One possible explanation for the slight increase of the *N* 1*s* peak is the presence of small but detectable amounts of impurities, such as titanium nitride (TiN) on the oxide surface.[17] Additionally, a small amount of Al 2*p* was also detected on the surfaces of the SLA-Ti samples, corroborating contamination by the Al_2O_3 grit-blasting particles. There is the possibility of the residual Al being released into the surrounding tissues, and this could have deleterious effects on the implant osseointegration. Moreover, the chemical heterogeneity resulting from the presence of Al and *N* may decrease the corrosion resistance of the Ti implant in a physiological environment.[18] Although they had an elemental composition similar to that of the other samples, the surfaces of the SLM-Ti samples had higher O and Ti contents and a lower C content, possibly due to the formation of a rutile layer after annealing. It has been reported that rutile is the most thermodynamically stable phase of crystalline TiO_2, and this is expected to afford better implant corrosion resistance and biocompatibility.[19]

Further, Figure 3(c) shows typical high-resolution X-ray diffraction (HR-XRD) patterns of the tested Ti samples, for detailed examination of the surface compositions. In the case of the cp-Ti and SLA-Ti samples, the major diffraction peaks occurred at 2θ values of 35.05°, 38.22°, 39.94° and 52.76°, which were indexed to the (100), (002), (101), and (102) planes of α-Ti (JCPDS card No. 44-1294), respectively. In agreement with the XPS results, the SLA-Ti samples also had additional diffraction peaks of modest intensity at 2θ values of 35.05°, 40.8° and 59.14°, which were attributed to the (111), (200), and (220) planes of TiN (JCPDS card No. 74-1214), respectively. In the case of the annealed SLM-Ti samples, prominent diffraction peaks were also observed at 2θ values of 27.21°, 54.06 ° and 56.38°, which corresponded to the (110), (301) and (112) planes of rutile TiO_2 (JCPDS card No. 77-0442). The α-Ti diffraction peaks in the SLM-Ti samples correspondingly appeared to shift to higher 2θ values. This should be related to the resultant residual stress from high cooling rate during SLM.

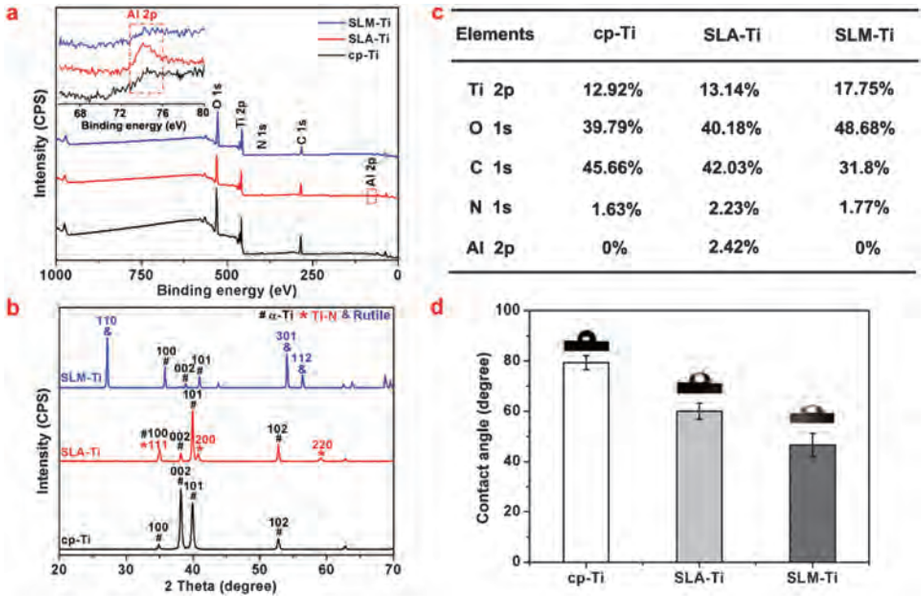

Elements	cp-Ti	SLA-Ti	SLM-Ti
Ti 2p	12.92%	13.14%	17.75%
O 1s	39.79%	40.18%	48.68%
C 1s	45.66%	42.03%	31.8%
N 1s	1.63%	2.23%	1.77%
Al 2p	0%	2.42%	0%

Fig. 3. XPS survey spectra (a), element composition (b), crystalline structures (c) and contact angle (d) for cp-Ti, SLA-Ti and SLM-Ti substrates. The insert in the upper-left corner of (a) shows the high-resolution spectrum of aluminum peaks (Al 2*p*) for all the substrates.

Measurement of the water contact angle is a convenient strategy for assessing the hydrophilic/hydrophobic properties of an implant surface. As shown in Figure 3(d), the pristine cp-Ti disk was relatively hydrophobic with a contact angle of about 79.38°, which decreased to an average of 60.03° after the SLA process. The increased surface wettability may be related to the formation of a micro/nano-texture during the SLA treatment.[20] The water contact angle of the SLM-Ti samples was even lower, at 46.57°. A positive correlation between surface roughness and wettability has been previously reported,[1,21] and the enhanced hydrophilicity of the SLM-Ti samples may be related to their assumed microtexture and increased surface roughness. The formation of a bioactive rutile layer on the samples by the annealing process, which facilitated rapid surface hydration, is another essential causal factor of the decreased contact angle.[16]

According to previous studies, the surface characteristics of implants, such as roughness, chemistry, and wettability, significantly influence cellular response and bone apposition.[16,22] As a feasible biomimetic method, SLM printing not only establishes a hierarchical microstructured surface with enhanced roughness and wettability, but also eliminates the contamination caused by Al_2O_3 particles and acid solution used for the SLA process. As previously reported, the increased surface roughness and hydrophilicity of the SLM-Ti samples observed in this study may work synergistically to yield a microenvironment that is suitable for hBMSCs attachment and proliferation, thus stimulating osteogenic differentiation, which would improve the success rates of implants.[23]

3.2. hBMSCs Adhesion and Proliferation on the Tested Ti Substrates

As the first phase of cell-implant interaction, better adhesion and proliferation enhance the quantity and quality of the newly formed bone around an implant, thus affording efficient osseointegration.[24] Hence, the suitability of the different Ti substrates for rapid cell adhesion and spreading was carefully analyzed by immunofluorescence staining over 24 h, which is deemed as the "decisive period" for cell attachment after an implantation. For all the Ti substrates (Fig. 4(a)), the seeding cells exhibited typical morphological changes comprising cell attachment, filopodium growth, cytoplasmic webbing, and flattening of cell mass,[25] similar to the case of the TCP control. After 6 h of incubation, only a small population of spindle-like hBMSCs were observed on the smooth surfaces of the cp-Ti samples, and most of the cells were generally round with few and short pseudopodia. In the case of the SLM-Ti and SLA-Ti samples, more triangular or polygonal cells with better cytoplasmic extensions were detected on their surfaces. Further, with increasing culturing duration of the SLM-Ti samples, the cells on their surfaces assumed more polygonal or flatter morphologies and anchored themselves to the surface through longer dendritic filopodia, indicating enhanced attachment.

To further explore the long-term cell response, the hBMSCs proliferation was examined by CCK-8 assays after 1, 4, and 7 days. Despite all the Ti substrates being inferior to the TCP substrate, the cells apparently proliferated on the former throughout the entire observation period (Fig. 4(b)). In addition, the SLM-Ti and SLA-Ti samples exhibited higher optical densities compared to the cp-Ti samples

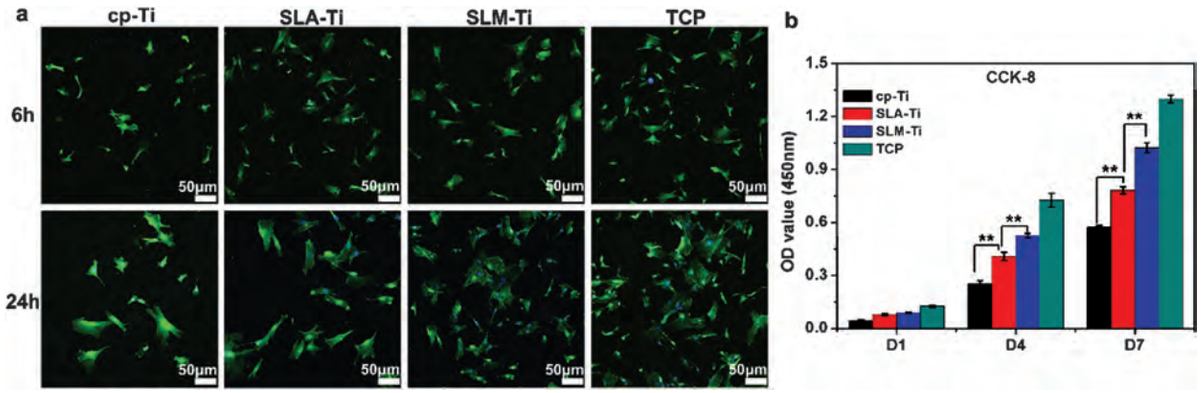

Fig. 4. Cell adhesion and proliferation of the hBMSCs cultured on the cp-Ti, SLA-Ti, SLM-Ti and TCP (control) substrates. (a) Visualization of the cytoskeleton (green, labeled with FITC-phalloidin) and cell nuclei (blue, counterstained with DAPI) after 6 h and 24 h of seeding. Scale bar: 50 μm. (b) The cell proliferation was evaluated by CCK-8 assay after 1, 4, and 7 days incubation ($n = 3$, $^{**}p < 0.01$).

($p < 0.01$) after 4 and 7 days of incubation, indicating that the increasing roughness and hydrophilicity was beneficial to cell proliferation. More importantly, the numbers of the hBMSCs attached to the SLM-Ti samples were about 1.29 and 1.31 times those for the SLA-Ti samples after 4 and 7 days, respectively. These results indicate that the SLM-printed substrates exhibited better cytocompatibility compared to the traditionally SLA-treated plates. Artificial implants with good biocompatibility ideally guarantee bonding with bone.

Previous works have posited that a rough and hydrophilic surface enhances adsorption of functional proteins, which are essential prerequisites for cell adhesion and proliferation.[16] Under the current experimental conditions, better hBMSCs adhesion and proliferation were observed on the SLM-printed substrates, substantiating the positive effect of roughness and wettability. The results are in quantitative agreement with reports that suggest that surface roughness ranging from 0.5 to 8.5 μm enhances cell behavior.[26,27] However, other researchers have insisted that Ra values of 1–2 μm are optimal, and that an overly low or overly high roughness may have a negative effect.[24,28] Further investigation of SLM-printed implants is thus required to fully establish the suitable physicochemical properties.

3.3. Osteogenic Differentiation of hBMSCs on the Tested Ti Substrates

To predict early *in vitro* osteogenesis, the hBMSCs cultured on the tested Ti substrates were assessed for ALP activity relative to the TCP control. The qualitative

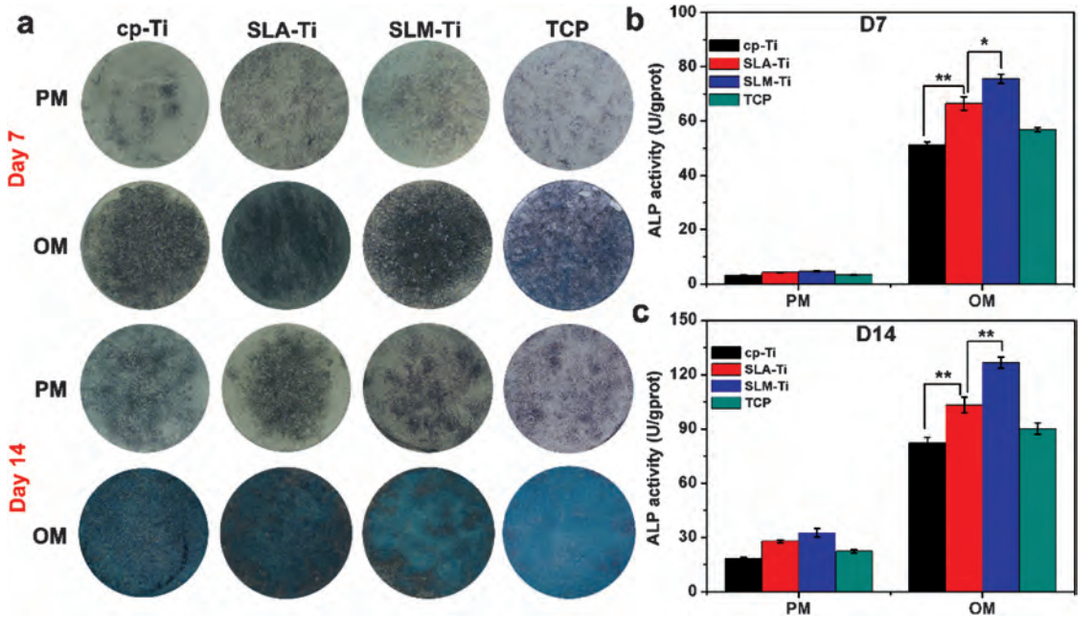

Fig. 5. Alkaline phosphatase (ALP) staining (a) and quantification (b and c) of hBMSCs cultured on cp-Ti, SLA-Ti, SLM-Ti and TCP surfaces for 7 and 14 days ($n = 3$, $^{*}p < 0.05$; $^{**}p < 0.01$).

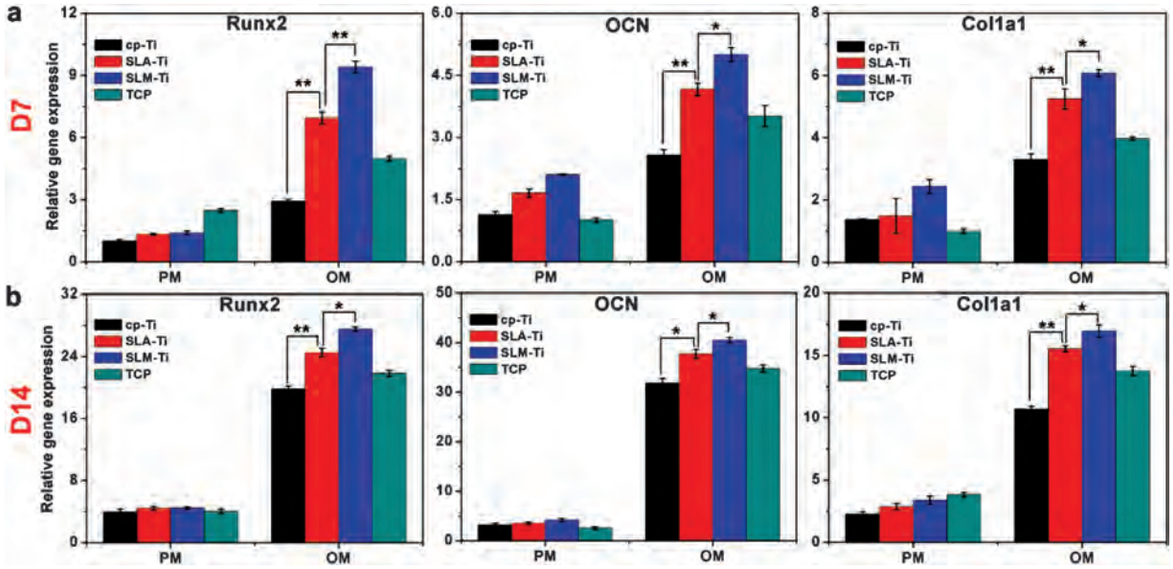

Fig. 6. The expression of osteogenic genes (Run × 2, OCN, Col1a1) in hBMSCs cultured on on cp-Ti, SLA-Ti, SLM-Ti and TCP surfaces for 7 and 14 days ($n = 3$, $^{*}p < 0.05$; $^{**}p < 0.01$).

(Fig. 5(a)) and quantitative (Fig. 5(b)) results showed no significant differences among the cells in the PM. However, after culturing in OM, increased ALP staining was observed (Fig. 5(a)), and there was also an apparently increased ALP expression as early as 7 days, and this continued into the 14th day (Figs. 5(b–c)). During the entire assay period, the ALP activities for the SLM and SLA samples were significantly higher than those for the planar control samples ($p < 0.01$), suggesting that surface topography stimulated and effectively supported osteogenesis. Further, the SLM-Ti samples induced more intensive expression than the other samples, especially after 14 days, providing the best conditions for early osteogenic differentiation of the hBMSCs.

In-depth molecular-level investigation is also instrumental to better understand the interactions between Ti substrates and hBMSCs. Consequently, we further monitored the variations in the expressions of the osteogenesis-related genes (Run × 2, OCN, and Col1a1) over 7 and 14 days. Run × 2 is the master transcription factor and facilitator of the osteogenic progress,[29] enabling the up-regulation of various downstream bone-related genes such as Col1a1 (an indicator of the production of organic bone matrix)[30] and OCN (an indicator of the mineralization of organic bone matrix).[30] The relative expressions of these genes can thus be used to assess the initial performance of an implant and the biological reaction of tissues.

As can be seen from Figure 6, there were almost no statistical differences among the sample groups for PM culturing. In the case of OM culturing, the expression of the osteo-special genes were substantially up-regulated for all the groups, with those for the SLA-Ti and SLM-Ti samples significantly higher for both considered durations ($p < 0.01$). It is noteworthy that the expression of OCN for the SLM-Ti samples was up-regulated approximately 40-fold after 14 days, and was 1.08 and 1.29 times those for the SLA-Ti and cp-Ti samples, respectively ($p < 0.05$). The changes in the expressions of the other two genes (Run × 2 and Col1a1) correlated well with that of OCN for all the examined sample groups. These observations indicate the promotion of osteogenesis by an SLM-printed substrate.

Extracellular calcium deposition at a late stage is another critical indicator for osteogenesis, and was investigated in this study by ARS staining and mineralization assays after 21 days of culturing (Fig. 7). There was obvious increased mineralization in the OM-treated samples, as revealed by the more intense red staining and higher ODs. In addition, the SLM substrates had more pronounced ARS-positive areas than the others, with only scanty calcium sediments observed on the surfaces of the cp-Ti samples. The results of the mineralization assays also revealed that the OM-cultured SLM substrates were more mineralized than the others, including the SLA substrates ($p < 0.05$). The observed higher calcium deposition for the SLM-Ti samples is consistent with previous reports and evidences the promotion of osteogenic differentiation of hBMSCs by the samples.

The overall observations of the present *in vitro* study clearly demonstrated that the superficial properties of the SLM substrates were beneficial for the expression of different signal molecules of osteogenesis, as represented by the up-regulated ALP activity, the expression of osteo-related genes, and calcium deposition. The osseointegration progress was closely associated with osteogenic differentiation and subsequent mineralization,

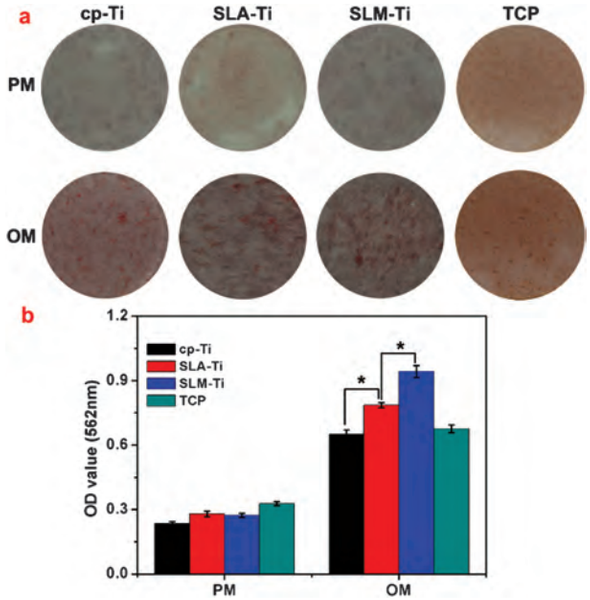

Fig. 7. Alizarin Red S staining (a) and mineralization assay (b) of hBMSCs cultured on cp-Ti, SLA-Ti, SLM-Ti and TCP surfaces on 21 days ($n = 3$, $^*p < 0.05$).

and SLM-based implants with optimal osteophilic characteristics are thus expected to stimulate conductive bone apposition. Further *in vivo* scientific and clinical validation is, however, required to confirm the efficacy of SLM-printed implants in this regard.

4. CONCLUSION

In this study, SLM substrates with surface properties suitable for implants were successfully fabricated, and their *in vitro* biofunctionalities were systematically estimated and compared with conventional SLA-treated samples. The overall results of the laboratory experiments clearly showed that the SLM substrates exhibited more favorable roughness, hydrophilicity, cytocompatibility, and cell interaction, as demonstrated by better cell adhesion, proliferation, and osteogenic differentiation. The findings of this study afford deeper insight and understanding of SLM-based implants, and offer critical guidance for the design of such implants with optimal superficial and biological properties, which are expected to improve the prospects of implant dentistry.

Conflict of Interest

No conflicts of interest, financial or otherwise, were declared by any of the authors.

Acknowledgments: This work was supported by the National Natural Science Foundation of China, Grant number 81300851, which was awarded to Yuwei Wu, the Beijing Municipal Natural Science Foundation, Grant number Z151100003715007, which was awarded to Zhihui Tang, and the National Key Research and Development Program of China, Grant number 2016YFB1101200, which was awarded to Zhihui Tang. We want to thank Ming Li for his assistance with preparation of this manuscript.

References and Notes

1. V. K. Truong, R. Lapovok, Y. S. Estrin, S. Rundell, J. Y. Wang, C. J. Fluke, R. J. Crawford, and E. P. Ivanova, *Biomaterials* 31, 3674 (**2010**).
2. D. K. Pattanayak, A. Fukuda, T. Matsushita, M. Takemoto, S. Fujibayashi, K. Sasaki, N. Nishida, T. Nakamura, and T. Kokubo, *Acta Biomater.* 7, 1398 (**2011**).
3. E. W. Zhang, Y. B. Wang, K. G. Shuai, F. Gao, Y. J. Bai, Y. Cheng, X. L. Xiong, Y. F. Zheng, and S. C. Wei, *Biomed. Mater.* 6, 025001 (**2011**).
4. S. Li, J. Ni, X. Liu, X. Zhang, S. Yin, M. Rong, Z. Guo, and L. Zhou, *J. Biomed. Mater. Res. B Appl. Biomater.* 100, 1587 (**2012**).
5. G. L. Yang, F. M. He, X. F. Yang, X. X. Wang, and S. F. Zhao, *Oral Surg. Oral Med. Oral Pathol. Oral Radiol. Endod.* 106, 516 (**2008**).
6. L. Le Guehennec, M. A. Lopez-Heredia, B. Enkel, P. Weiss, Y. Amouriq, and P. Layrolle, *Acta Biomater.* 4, 535 (**2008**).
7. H. Attar, M. Calin, L. C. Zhang, S. Scudino, and J. Eckert, *Mater. Sci. Eng. A Struct.* 593, 170 (**2014**).
8. A. Fukuda, M. Takemoto, T. Saito, S. Fujibayashi, M. Neo, D. K. Pattanayak, T. Matsushita, K. Sasaki, N. Nishida, T. Kokubo, and T. Nakamura, *Acta Biomater.* 7, 2327 (**2011**).
9. L. C. Zhang and H. Attar, *Adv. Eng. Mater.* 18, 463 (**2016**).
10. Y. J. Liu, S. J. Li, H. L. Wang, W. T. Hou, Y. L. Hao, R. Yang, T. B. Sercombe, and L. C. Zhang, *Acta Mater.* 113, 56 (**2016**).
11. L. E. Murr, E. V. Esquivel, S. A. Quinones, S. M. Gaytan, M. I. Lopez, E. Y. Martinez, F. Medina, D. H. Hernandez, E. Martinez, J. L. Martinez, S. W. Stafford, D. K. Brown, T. Hoppe, W. Meyers, U. Lindhe, and R. B. Wicker, *Mater. Charact.* 60, 96 (**2009**).
12. P. Li, D. H. Warner, A. Fatemi, and N. Phan, *Int. J. Fatigue* 85, 130 (**2016**).
13. N. Dai, L. C. Zhang, J. Zhang, Q. Chen, and M. Wu, *Corros. Sci.* 102, 484 (**2016**).
14. N. Dai, L. C. Zhang, J. Zhang, X. Zhang, Q. Ni, Y. Chen, M. Wu, and C. Yang, *Corros. Sci.* 111, 703 (**2016**).
15. S. A. Yavari, J. van der Stok, Y. C. Chai, R. Wauthle, Z. T. Birgani, P. Habibovic, M. Mulier, J. Schrooten, H. Weinans, and A. A. Zadpoor, *Biomaterials* 35, 6172 (**2014**).
16. L. Bacakova, E. Filova, M. Parizek, T. Ruml, and V. Svorcik, *Biotechnol. Adv.* 29, 739 (**2011**).
17. J. H. Park, Z. Schwartz, R. Olivares-Navarrete, B. D. Boyan, and R. Tannenbaum, *Langmuir* 27, 5976 (**2011**).
18. L. L. Guehennec, A. Soueidan, P. Layrolle, and Y. Amouriq, *Surface Treatments of Titanium Dental Implants for Rapid Osseointegration, Dent. Mater.* 23, 844 (**2007**).
19. J. Forsgren, F. Svahn, T. Jarmar, and H. Engqvist, *Acta Biomater.* 3, 980 (**2007**).
20. Z. Lin, Y. Wang, D. N. Wang, B. H. Zhao, and J. C. Li, *Surf. Coat. Tech.* 228, S131 (**2013**).
21. J. W. Park, Y. J. Kim, C. H. Park, D. H. Lee, Y. G. Ko, J. H. Jang, and C. S. Lee, *Acta Biomater.* 5, 3272 (**2009**).
22. R. A. Gittens, T. McLachlan, R. Olivares-Navarrete, Y. Cai, S. Berner, R. Tannenbaum, Z. Schwartz, K. H. Sandhage, and B. D. Boyan, *Biomaterials* 32, 3395 (**2011**).
23. K. M. Hotchkiss, G. B. Reddy, S. L. Hyzy, Z. Schwartz, B. D. Boyan, and R. Olivares-Navarrete, *Acta Biomater.* 31, 425 (**2016**).
24. W. C. Chen, Y. S. Chen, C. L. Ko, Y. Lin, T. H. Kuo, and H. N. Kuo, *Mater. Sci. Eng. C Mater. Biol. Appl.* 37, 305 (**2014**).

25. L. Ma, H. Qin, C. Cheng, Y. Xia, C. He, C. X. Nie, L. R. Wang, and C. S. Zhao, *J. Mater. Chem. B* 2, 363 **(2014)**.
26. M. M. Shalabi, A. Gortemaker, M. A. Van't Hof, J. A. Jansen, and N. H. Creugers, *J. Dent. Res.* 85, 496 **(2006)**.
27. B. A. van Oirschot, R. M. Eman, P. Habibovic, S. C. Leeuwenburgh, Z. Tahmasebi, H. Weinans, J. Alblas, G. J. Meijer, J. A. Jansen, and J. J. van den Beucken, *Acta Biomater.* 37, 195 **(2016)**.
28. Y. Deng, X. Liu, A. Xu, L. Wang, Z. Luo, Y. Zheng, F. Deng, J. Wei, Z. Tang, and S. Wei, *Int. J. Nanomedicine* 10, 1425 **(2015)**.
29. H. K. Kim, J. H. Kim, D. S. Park, K. S. Park, S. S. Kang, J. S. Lee, M. H. Jeong, and T. R. Yoon, *Biomaterials* 33, 7057 **(2012)**.
30. G. Kaur, M. T. Valarmathi, J. D. Potts, and Q. Wang, *Biomaterials* 29, 4074 **(2008)**.